

# Recovery efficiency and characteristics of long core by CO<sub>2</sub> flooding in low permeability sandstone reservoirs

Feng Tian<sup>1,2</sup>, Tiantai Li<sup>1\*</sup>

<sup>1</sup> School of Petroleum Engineering, Xi'an Shiyou University, Xi'an 710065, China

<sup>2</sup> School of Petroleum Engineering, China University of Petroleum, Beijing 102249, China

**Abstract**—CO<sub>2</sub> flooding is an economical and efficient enhanced oil recovery technology, however, it is difficult for conventional short core experiments to provide accurate parameters for the later on-site optimization scheme. In this paper, on the basis of long core flooding experiments and applying NMR technology, we quantitatively evaluated the recovery efficiency and remaining oil distribution characteristics by CO<sub>2</sub> in low-permeability sandstone reservoirs from a microscopic perspective, and explored the potential of CO<sub>2</sub> flooding in low-permeability sandstone reservoirs. Results showed that with the CO<sub>2</sub> injection pressure increase, the recovery efficiency of the long core increased and the ultimate recovery was 65.3%. Recovery efficiency of short cores at the inlet, middle and outlet decreases successively, but the change range was not large, and all of them are around the recovery efficiency of long core. In addition, at low injection pressure, almost all CO<sub>2</sub> went into the larger pores to replace oil. As increased pressure, the oil started to be produced from the smaller pores, but at 22 MPa, the recovery efficiency in larger pores (76.88%-83.38%) was still higher than that of smaller pores (68.73%-72.74%). Which provided a guide for optimizing the CO<sub>2</sub> enhanced oil recovery method in the field.

## 1. Introduction

In recent years, low permeability resources have become a major part of global crude oil supply. As a result of the poor physical properties, thin pore throats, with the proposed start pressure gradient, etc., there are some problems in conventional waterflooding development of low permeability reservoir, such as high waterflooding pressure, rapid rise of water content, high cost of waterflooding, serious reduction of permeability and low productivity, which make it very difficult to stabilize and increase oil production [1].

CO<sub>2</sub> gas has advantages of strong injection capacity, large expansion coefficient, good miscibility with crude oil, etc., and can significantly enhance oil recovery [2-4]. At present, the influential factors and characteristics of CO<sub>2</sub> flooding have been extensively studied. However, it is difficult for conventional short core experiments to provide accurate parameters for the later on-site optimization scheme, so some scholars use long core experiments to evaluate the oil recovery effect [5, 6].

In recent years, nuclear magnetic resonance (NMR) technology is applied frequently in oil and gas fields to evaluate recovery efficiency and residual oil distribution characteristics [7, 8], but few studies have combined NMR technology with long core flooding experiments. In this paper, on the basis of long core flooding

experiments and applying NMR technology, we quantitatively evaluated the recovery efficiency and remaining oil distribution characteristics by CO<sub>2</sub> in low-permeability sandstone reservoirs from a microscopic perspective, and explored the potential of CO<sub>2</sub> flooding in low-permeability sandstone reservoirs, which provided a guide for optimizing the CO<sub>2</sub> enhanced oil recovery method in the field.

## 2. Experimental section

### 2.1 Preparation of long core

In order to complete the single pipe core flooding experiment, the conventional short core is arranged by harmonic average method to prepare long core [6]. Each core is connected to each other with filter paper for eliminating the end effect of rock. The information of the spliced cores is shown in Table 1.

The steps of long core preparation are as follows:

① Long core permeability can be calculated from equation (1).

$$\frac{\bar{L}}{\bar{K}} = \frac{L_1}{K_1} + \frac{L_2}{K_2} + \dots + \frac{L_i}{K_i} + \dots + \frac{L_n}{K_n} = \sum_{i=1}^n \frac{L_i}{K_i} \quad (1)$$

\* ttli@xsyu.edu.cn

$\bar{K}$  is long core permeability,  $K_1, K_2 \dots K_n$  are short core permeability, respectively;  $\bar{L}$  is long core length,

$L_1, L_2 \dots L_n$  are short core length, respectively.

**Table 1.** The information of the spliced cores.

Number of long core	Number of short core	Length /cm	Diameter /cm	Permeability / $10^{-3}\mu\text{m}^2$	Porosity /%
L#	S1#	6.72	25.3	8.48	15.24
	S2#	6.21	25.3	7.40	14.94
	S3#	6.25	25.2	8.68	14.89
	S4#	6.58	25.3	7.31	14.33
	S5#	6.39	25.3	8.69	15.58
	S6#	6.54	25.3	8.74	15.75
	S7#	6.93	25.2	7.24	12.85
	S8#	6.35	25.3	8.81	15.54
	S9#	6.21	25.2	7.22	14.12
	S10#	6.65	25.2	7.19	14.10
	S11#	7.16	25.3	7.18	13.86
	S12#	6.31	25.3	9.69	15.89
	S13#	6.32	25.3	7.14	14.04
	S14#	5.76	25.2	9.90	15.63
	S15#	5.58	25.3	6.87	11.99
	S16#	6.49	25.2	10.23	17.86
Average/Su		102.45	25.26	8.03	14.79

② By comparing the permeability of conventional short core with that of long core, the short core placed first at the outlet end is the core whose permeability is the closest to that of long core.

③ Continue to repeat steps ① and ②, the remaining short cores were sequentially arranged into the core holder.

## 2.2 Preparation of experimental oil, formation water and CO<sub>2</sub> gas

The experimental oil was prepared with crude oil samples from Chang-2 reservoir of Dingbian Oilfield and kerosene in proportion to the volume of 1:1, which has a viscosity of 7.1 mPa·s and a minimum miscibility pressure (MMP) of 17.8 MPa with CO<sub>2</sub>. The experimental formation water was prepared based on the actual water quality monitoring data of Chang-2 reservoir in Dingbian Oilfield, and the salinity is 25000mg/L. The purity of CO<sub>2</sub> gas is 99.9%.

## 2.3 Experimental setup

As shown in Figure 1, the power is provided by the syringe pump, which is capable of continuously providing high accuracy, constant speed or constant pressure fluid for a long time, and it has a maximum working pressure of 150 MPa and an accuracy of 0.001 mL/min. The experimental temperature is maintained by the thermostatic oven, which can provide a maximum temperature of 200°C with an accuracy of 0.1°C. The maximum core length that the long core holder can hold is 120 cm and the maximum pressure it can hold is 35 MPa. The produced fluid is separated by the oil and gas separator and then enters the gas flow meter, which has an accuracy of 0.001 mL.

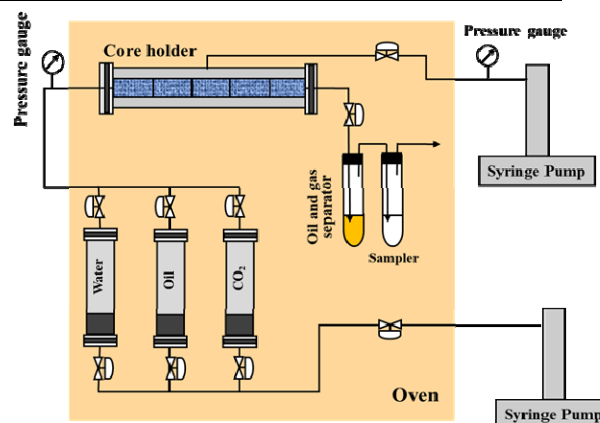


**Figure 1.** Schematic of experimental flow.

## 2.4 Experimental steps

① Core preparation. The selected core were deeply cleaned with petroleum ether and benzene for 120h, and the cleaned core were dried in the thermostatic oven at 120 °C for 24 h. Then the measurements of length, diameter and permeability of the cores were taken, as shown in Table 1. Dry the core after the test (120 °C, 24 h). The short cores were spliced into long cores by harmonic average method, and cores were renumbered in order of arrangement, as shown in Table 1.

② Saturated formation water. The simulated formation water is configured according to reservoir formation water component. In order to completely saturate the core with simulated formation water, a constant flow rate of 0.05 mL/min was used to inject formation water into the core until the injection volume exceeded twice the volume of the core. Also, the core porosity was calculated, as shown in Table 1. Then, the NMR T<sub>2</sub> spectrum were acquired for the core saturated with formation water.

③ Saturated  $Mn^{2+}$  solution. The  $Mn^{2+}$  solution was configured with concentration of 15000 mg/L, and a constant flow rate of 0.05 mL/min was used to inject  $Mn^{2+}$  solution into the core until the injection volume was 3-4 PV. Then, the NMR  $T_2$  spectrum were acquired for the core after  $Mn^{2+}$  solution flooding to ensure the elimination of the water signal.

④ Saturated experimental oil. The original oil-water distribution was established by injection of the experimental oil into the core at a constant flow rate of 0.05 mL/min until the oil content of the outlet liquid was 100%. Then, the NMR  $T_2$  spectrum were acquired for the core saturated with experimental oil.

⑤  $CO_2$  flooding. The injection pressure was stabilized at 7.2 MPa, 12 MPa, 17 MPa and 22 MPa by controlling the backpressure valve, respectively, and a constant flow rate of 0.05 mL/min was used to inject  $CO_2$  into the core to flooding oil until there was no crude oil in the outlet liquid. Then, the NMR  $T_2$  spectrum were acquired for the core after  $CO_2$  flooding.

⑥ After flooding, the cores were re-cleaned and dried according to step ①. Then, change the injection pressure and repeat steps ② - ⑤.

### 3. Results and analysis

#### 3.1 Recovery efficiency

The recovery efficiency of long core (core L#) and short core at the inlet (core S1#), middle (core S8#) and outlet (core S16#) were calculated respectively, where the

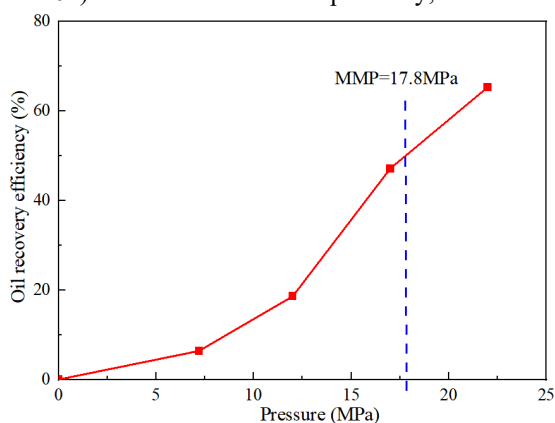


**Figure 2.** The relationship between recovery efficiency of core L# and pressure.

#### 3.2 Remaining oil distribution characteristics

The  $T_2$  spectrum of short core at the inlet (core S1#), middle (core S8#) and outlet (core S16#) were selected for analysis recovery efficiency and remaining oil distribution characteristics in larger and smaller pores, as shown in Figure 4-6. The variation trend of  $T_2$  spectrum and recovery efficiency in larger and smaller pores for core S1#, S8# and S16# are similar.

At 7.2 MPa, basically all  $CO_2$  entered the larger pores, the  $T_2$  amplitude decreased significantly in larger pores, the recovery efficiency is 6.71%~8.73%. While

recovery efficiency of the short cores were calculated by NMR  $T_2$  spectrum and the recovery efficiency of the long core was calculated by the volume of produced fluid.

As shown in Figure 2, with the  $CO_2$  injection pressure increase, the recovery efficiency of core L# increases. At 7.2MPa, the recovery efficiency is only 6.4%. As the pressure increases to MMP and continues to increase, the potential of the core L# is activated, and the recovery efficiency increases sharply to 65.3% at 22 MPa. This is because injection pressure increases, the solubility of  $CO_2$  in crude oil increases, which makes crude oil viscosity decrease, capillary pressure decrease, and crude oil flow more easily. Moreover, the injection pressure reaches MMP, the  $CO_2$  flooding mechanism is transformed due to its greatly enhanced extraction capacity and greatly reduced interfacial tension with crude oil, resulting in significantly higher recovery efficiency.

As shown in Figure 3, with the  $CO_2$  injection pressure increase, the recovery efficiency of core S1#, S8# and S16# increases, which is the similar as that of core L#. In addition, the recovery efficiency of core S1#, S8# and S16# decreased successively, but the change range was not large, and all of them are around recovery efficiency of core L#. This is because  $CO_2$  replaced the crude oil in core S1#, S8#, and S16# successively during the flooding process. The flooding time was long enough for  $CO_2$  to fully replace the crude oil in the core L#. Therefore, there is little difference between the final recovery efficiency of inlet and outlet.

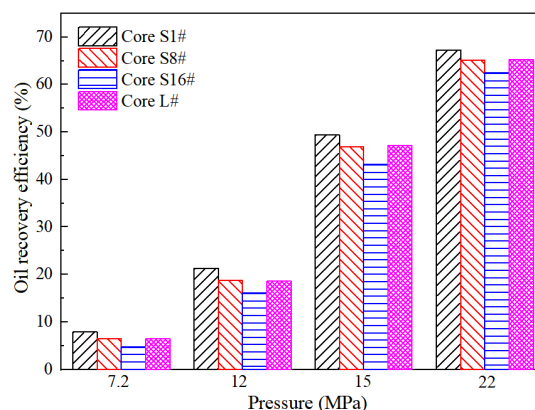


**Figure 3.** The relationship between recovery efficiency of core S1#, S8#, S16# and L# and pressure.

the  $T_2$  amplitude changed little in smaller pores, the recovery efficiency is only 1.71%~2.1%. When the pressure increased to 12 MPa, the  $T_2$  amplitude decreased significantly in smaller pores, indicating that the crude oil also started to be produced in the smaller pores at this stage, but the recovery efficiency in the smaller pores (11.07%~14.33%) was still significantly lower than that in the larger pores (18.97%~21.63%). This is because  $CO_2$  will preferentially enter the larger pores with low resistance, and only when the pressure accumulated in the larger pores reaches enough to overcome the capillary pressure will it enter the smaller

pores and replace the crude oil. As the pressure increases to MMP and continues to increase, the  $T_2$  amplitude significantly reduced both in larger and smaller pores, and the recovery efficiency is significantly enhanced. This is because at this stage, the extraction capacity of  $CO_2$  is significantly enhanced and the interfacial tension disappears, making it easier for  $CO_2$  to enter the smaller pores with higher original resistance and replace crude

oil, which greatly improves the recovery efficiency. In addition, it also can be seen that at 22 Mpa, the recovery efficiency in larger pores (76.88%-83.38%) was still greater than that in smaller pores (68.73%-72.74%). This is mainly because even if at miscible stage,  $CO_2$  will preferentially enter larger pores, and the miscible flooding is formed in larger pores, then which diffuse to the surrounding pores.

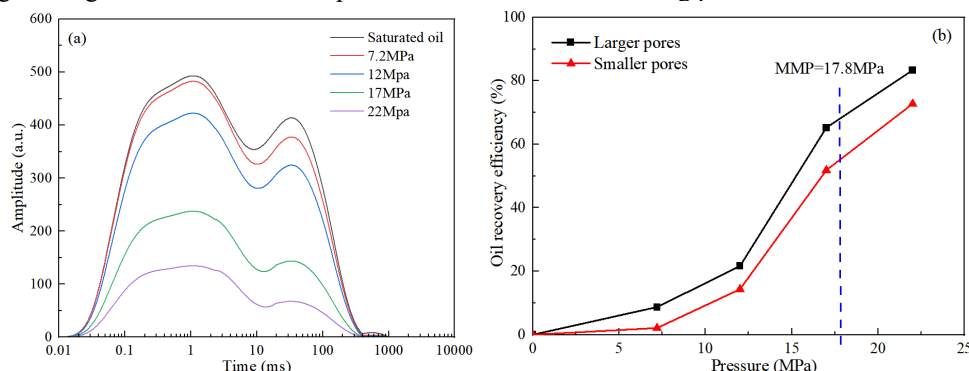


**Figure 4.** (a)  $T_2$  spectrum distribution and (b) recovery efficiency in larger and smaller pores of core S1# under different pressures.

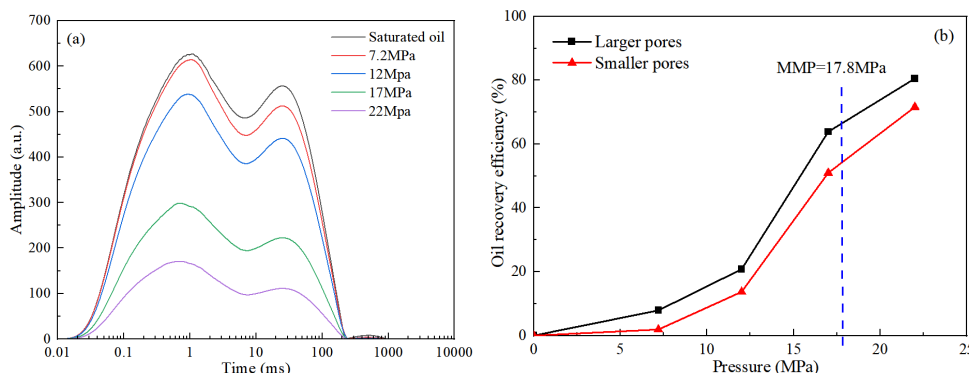


**Figure 5.** (a)  $T_2$  spectrum distribution and (b) recovery efficiency in larger and smaller pores of core S8# under different pressures.

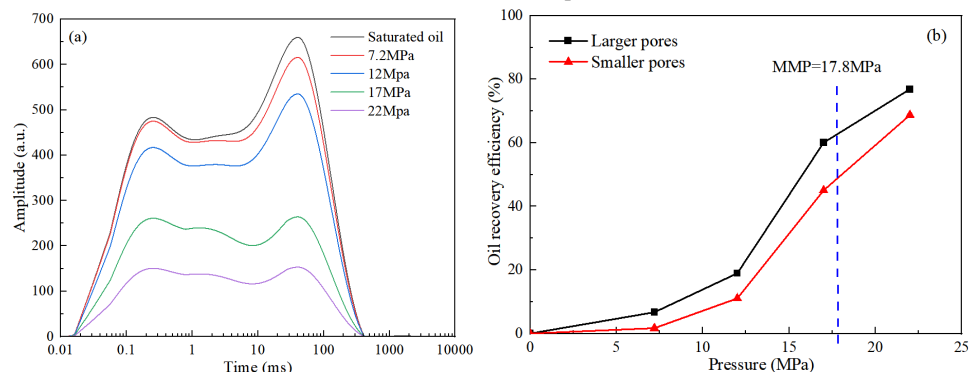


**Figure 6.** (a)  $T_2$  spectrum distribution and (b) recovery efficiency in larger and smaller pores of core S16# under different pressures.

## 4. Conclusion

In this paper, on the basis of long core flooding experiments and applying NMR technology, the recovery efficiency and remaining oil distribution characteristics by  $CO_2$  flooding in low-permeability sandstone reservoirs were quantitatively evaluated from a microscopic perspective, and the potential of  $CO_2$  flooding in low-permeability sandstone reservoirs was explored, which provided a guide for optimizing the  $CO_2$

enhanced oil recovery method in the field. The conclusions are obtained as below:

- (1) The recovery efficiency of long core increases with the  $CO_2$  injection pressure increase, and the ultimate recovery was 65.3%.
- (2) The recovery efficiency of short core at the inlet, middle and outlet decreased successively, but the change range was not large, and all of them are around recovery efficiency of long core.
- (3) At low injection pressure, almost all  $CO_2$  went into the larger pores to replace oil. As increased pressure,

the oil started to be produced from the smaller pores, but at 22 MPa, the recovery efficiency in larger pores (76.88%-83.38%) was still higher than that of smaller pores (68.73%-72.74%). Which provided a guide for optimizing the CO<sub>2</sub> enhanced oil recovery method in the field.

## References

1. Hu, W., Wei, Y., Bao, J, (2018) Development of the theory and technology for low permeability reservoirs in China. *Pet. Explor. Dev.*, 45(4), 685-697.
2. Yu, W., Lashgari, H. R., Wu, K., et al. (2015) CO<sub>2</sub> injection for enhanced oil recovery in Bakken tight oil reservoirs. *Fuel*, 159, 354-363.
3. Fakher, S., Imqam, A. (2020) Application of carbon dioxide injection in shale oil reservoirs for increasing oil recovery and carbon dioxide storage. *Fuel*, 265, 116944.
4. Huang, X., Ni, J., Li, X., et al. (2020) Characteristics and influencing factors of CO<sub>2</sub> flooding in different microscopic pore structures in tight reservoirs. *Acta Pet. Sin.*, 41(7), 853.
5. Li, F., Yang, S., Chen, H., et al. (2014) Long core physical simulation for CO<sub>2</sub> flooding in low permeability reservoir. *Int. J. Oil, Gas Coal Technol.*, 8(3), 251-261.
6. Zhang, G., Li, D., Jia, G., et al. (2022) Laboratory test on CO<sub>2</sub> injection displacement in long cores of Huabei oilfield. *Pet. Geol. Eng.*, 36(06): 77-81.
7. Zhu, C., Sheng, J. J., Etehadavakkol, A., et al. (2019) Numerical and experimental study of enhanced shale-oil recovery by CO<sub>2</sub> miscible displacement with NMR. *Energy Fuels*, 34(2), 1524-1536.
8. Huang, X., Li, A., Li, X., et al. (2019) Influence of typical core minerals on tight oil recovery during CO<sub>2</sub> flooding using the nuclear magnetic resonance technique. *Energy Fuels*, 33(8), 7147-7154.